Bull. Mater. Sci., Vol. 35, No. 5, October 2012, pp. 751–757. © Indian Academy of Sciences.

Preparation of cadmium-doped ZnO thin films by SILAR and their characterization

S MONDAL and P MITRA*
Department of Physics, University of Burdwan, Burdwan 713 104, India

MS received 9 May 2011; revised 4 July 2011

Abstract. **Cadmium-doped zinc oxide (Cd : ZnO) thin films were deposited from sodium zincate bath following a chemical dipping technique called successive ion layer adsorption and reaction (SILAR). Structural characterization by X-ray diffraction reveals that polycrystalline nature of the films increases with increasing cadmium incorporation. Particle size evaluated using X-ray line broadening analysis shows decreasing trend with increasing cadmium impurification. The average particle size for pure ZnO is 36·73 nm and it reduces to 29·9 nm for 10% Cd:ZnO, neglecting strain broadening. The strong preferred *c*-axis orientation is lost due to cadmium doping and degree of polycrystallinity of the films also increases with increasing Cd incorporation. Incorporation of cadmium was confirmed from elemental analysis using EDX. The optical bandgap of the films decreases with increasing Cd dopant. The value of fundamental absorption edge is 3·18 eV for pure ZnO and it decreases to 3·11 eV for 10% Cd:ZnO.**

Keywords. **SILAR; Cd:ZnO thin film; X-ray line broadening; SEM; optical bandgap.**

1. Introduction

Zinc oxide possesses a unique position among semiconducting material owing to its superior and diverse properties such as piezoelectricity, chemical stability, biocompatibility, high catalytic activity in different gas ambient, optical transparency in the visible region and high voltage–current nonlinearity etc (Maiti *et al* 2007). Accordingly it has immense potential in different applications in photothermal conversion systems, heat mirrors, heterojunction solar cells, transparent electrodes, blue/UV light emitter device, solid state sensor, transducer (Maiti *et al* 2007; Suchea *et al* 2007; Vijayalakshmi *et al* 2008) etc. The interest in doping ZnO is to explore the possibility of tailoring its physical properties (Aktaruzzaman *et al* 1991). Since most of the device applications require the material in thin film form, various physical and chemical techniques have been employed to synthesize pure and doped ZnO films. Polycrystalline films of ZnO have been doped with various dopants (e.g. Al, Ni, Mn, Pd, Cu, Fe, Cd etc) (Bedir *et al* 2006; Mandal and Nath 2006; Ghosh *et al* 2008; Kumar *et al* 2008; Yakuphanoglu *et al* 2010; Al-zaidi *et al* 2011) to obtain improved physical properties. Although cadmium-doped ZnO is one of the promising candidates in the field of optoelectronics and also for the fabrication of ZnO based devices (Vijayalakshmi *et al* 2008), knowledge of the physical properties of Cd-doped ZnO was very limited until recent times. Cadmium oxide possesses cubic structure and a narrow direct bandgap of 2·3 eV, whereas ZnO possesses a wide bandgap of 3·2 eV (Dong *et al* 1997; Cao *et al* 2000). Hence, it is possible to modify the physical properties of ZnO upon mixing with CdO. In recent times, there are reports of Cd-doped ZnO either in thin film or nanostructured form with varying amounts of Cd incorporation (Choi *et al* 1996; Makino *et al* 2001; Gruber *et al* 2003; Wang *et al* 2005; Yogeeswaran *et al* 2006; Maiti *et al* 2007; Vijayalakshmi *et al* 2008; Yakuphanoglu *et al* 2010). Substitution of zinc ion by isoelectronic element cadmium has been reported by complicated physical processes such as combustion synthesis technique (Yogeeswaran *et al* 2006), pulsed laser deposition (PLD) (Makino *et al* 2001), metal–organic vapour phase epitaxy (MOVPE) (Gruber *et al* 2003), vapour–liquid–solid (VLS) (Wang *et al* 2005). Reports of cadmium-doped zinc oxide synthesized through chemical routes are relatively rare. Among the chemical techniques, sol–gel (Choi *et al* 1996; Maiti *et al* 2007; Yakuphanoglu *et al* 2010) and spray pyrolysis (Vijayalakshmi *et al* 2008) have been employed to deposit Cd-doped ZnO films. Chemical techniques are relatively simpler and cost effective.

In the present work, an attempt has been made to synthesize Cd-doped ZnO by a chemical dipping technique. In this technique, a glass substrate is dipped alternatively into beakers containing aqueous solutions or distilled water for the reaction to take place at the substrate surface. The substrate can be introduced into various reactants for a specific length of time depending on the nature and kinetics of the reaction. The immersion-reaction cycle can be repeated for any number of times, limited only by the inherent problems associated with the deposition technique and the substrate–thin film interface. The technique, initially developed by Call *et al* (1980) and Ristov *et al* (1987), was given the name, successive ion layer adsorption and reaction (SILAR) by

*Author for correspondence (mitrapartha1@rediffmail.com)

Nicolau *et al* (1990) since it involves adsorption of a layer of complex ion on the substrate followed by reaction of the adsorbed ion layer. SILAR deposition from aqueous solutions is a very promising method because of its simplicity and economy. The technique is, however, a relatively less used and studied one. The advantages of this method are its simplicity of working principle and low cost of apparatus. Earlier we have reported the synthesis of ZnO thin film (Chatterjee *et al* 1999; Mitra and Khan 2006) and Al-doped ZnO thin films by SILAR (Mondal *et al* 2008). The primary aim of the present work was to explore the possibility of utilizing SILAR to impurify ZnO thin film with Cd.

2. Experimental

Deposition of ZnO and Cd-doped ZnO was carried out from 0·1M sodium zincate (Na_2ZnO_2) solution and hot water bath. The sodium zincate bath used for deposition was prepared by adding sodium hydroxide (NaOH pellets, Merck, mol. wt 40·00) in zinc sulphate ($ZnSO_4{\cdot}7H_2O$, Merck, mol. wt 287·54) solution. pH of the zincate solution was 13·20. pH measurement was carried out in a systronics pH meter (Model 335). Cadmium doping was carried out by adding cadmium chloride ($CdCl_2{\cdot}H_2O$, GR grade, Loba Chemie, mol. wt 201·32) in sodium zincate bath.

Details of pure ZnO film deposition process from sodium or ammonium zincate bath has been reported earlier (Chatterjee *et al* 1999; Mitra and Khan 2006; Mondal *et al* 2008). Briefly, a pre-cleaned substrate (microscopic glass slide) was alternatively dipped in sodium zincate bath kept at room temperature and hot water bath maintained at ∼95–98 °C. The glass substrate was cleaned prior to deposition, by chromic acid followed by distilled water rinse and ultrasonic cleaning with equivolume acetone and alcohol. The cleaned substrate was tightly held in a holder so that only a requisite area for film deposition was exposed. Thus, the film deposition area could be easily varied by adjusting the holder arrangement. One set of dipping involves dipping in zincate bath for 2 s and 2 s in hot water bath. 50 dippings were performed for the present experiment. The cadmium concentration was varied up to 10% in the bath solution. The thickness for pure ZnO film measured gravimetrically (Mitra and Khan 2006; Mondal *et al* 2008) was ∼1·0 μm.

The phase identification and crystalline properties of the films were studied by X-ray diffraction (XRD) method employing a Philips PW 1830 X-ray diffractometer with CuKα radiation ($\lambda = 1{\cdot}5418$ Å). The experimental peak positions were compared with the standard JCPDS files and the Miller indices were indexed to the peaks. Scanning electron microscopy (SEM, Model S530, Hitachi, Japan) was used to study the surface morphology and to illustrate the formation of crystallites on the film surface. UV-VIS spectrophotometric measurements were performed by using a spectrophotometer (Shimadzu, UV-1800) at room temperature. The spectra were recorded by using a similar glass as a reference and hence the absorption due to the film only was obtained. The bandgap of the films was calculated from the absorption edge of the spectrum.

3. Results and discussion

The X-ray diffraction patterns of undoped ZnO and Cd-doped ZnO films are shown in figure 1. The diffraction pattern for undoped ZnO is shown in figure 1(a). Figures 1(b) and (c) show diffractograms for 5% and 10% Cd ZnO-doped films, respectively. The films were heat treated at 350 °C for 2 h prior to structural characterization. The materials were scanned in the range 20–60°. The 2θ variation was employed with a 0·05 degrees step and a time step of 1 s. Intensity in arbitrary units is plotted against 2θ in figure 1. It is seen from figure 1(a) that peaks appear at 31·6°, 34·35°, 36·20°, 47·55° and 56·55°. The diffractogram of the sample reveals that all the peaks are in good agreement with the JCPDS data belonging to hexagonal ZnO structure (Card No. 36-1451). The corresponding reflecting planes are (100), (002), (101), (102) and (110), respectively. The (002) peak appears with a maximum intensity at 34·35°. For 5% Cd:ZnO, peaks are obtained at 31·60°, 34·3°, 36·1°, 47·40° and 56·40° and the corresponding values for 10% Cd:ZnO films are 31·55, 34·25, 36·15, 47·45 and 56·40, respectively. Apart from ZnO characteristic peaks, no peaks that correspond to either cadmium, zinc or their complex oxides could be detected. This observation suggests that the films do not have any phase segregation or secondary phase formation as well as Cd incorporation into ZnO lattice.

It is evident from figure 1(a) that pure ZnO film has a polycrystalline structure with strong preferred orientation in the (002) direction. Compared with pure ZnO film, the intensity

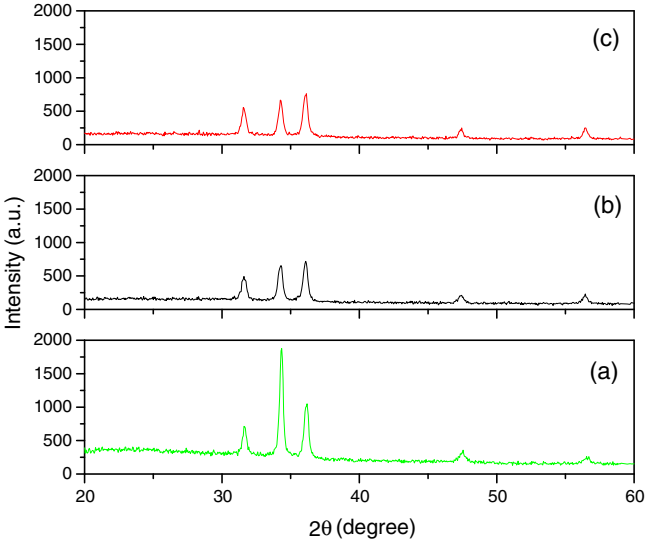

Figure 1. X-ray diffraction patterns of (**a**) 0 ZnO, (**b**) 5% Cd-doped ZnO and (**c**) 10% Cd-doped ZnO.

of (002) peak decreases for Cd:ZnO films. Also the relative intensity of (101) peak increases for Cd:ZnO films. Thus cadmium doping results in loss of preferred orientation along *c*-axis since (101) peak appears with maximum intensity in ZnO powders with no preferred orientation (Mitra and Khan 2006). Uilizing the X-ray diffraction data, the average particle/grain size was estimated by Scherrer formula (Klug and Alexander 1974; Gupta *et al* 2009):

$$D = \frac{k\lambda}{\beta \cos\theta}, \tag{1}$$

where λ is the wavelength of radiation used (1·542 Å for CuKα radiation used), k the Scherrer constant, β the full width at half maximum (FWHM) intensity of the diffraction peak for which the particle size is to be calculated, θ the diffraction angle of the concerned diffraction peak and D the crystallite dimension (or particle size). In Scherrer equation, β represents the broadening due to particle size alone. The experimentally observed broadening (β_0) is the total contribution from particle size broadening (β), instrumental broadening (β_i) and strain broadening (β_s). Ignoring strain broadening, we can write (Klug and Alexander 1974):

$$\beta = \beta_0 - \beta_i. \tag{2}$$

Diffraction data from standard silicon (Si) powder was used to measure the instrumental broadening (Patra *et al* 2011) at the observed peak positions.

X-ray line broadening analysis was carried out to evaluate FWHM (β) using computer software (MARQ2) (Jumin and Wang 2001; Ghosh *et al* 2009). The software utilizes Marquardt least-squares procedure for minimizing the difference between observed and simulated diffraction patterns. The peak-shape and intensity of reflection is modelled with a pseudo-Voigt (pV) analytical function, which is a combination of a Gaussian and a Lorentzian function. The background intensity is subtracted by fitting the background with a suitable linear or polynomial function. A typical plot of MARQ2 analysis for undoped ZnO sample is shown in figure 2. The dotted curve represents the experimental intensity data (I_o) and the continuous curve represents the calculated (simulated) intensity data (I_c). The difference plot ($I_c - I_o$) is shown at the bottom.

From the values of β_0 obtained using MARQ2 fitting and the corresponding values of instrumental broadening, β_i, β was calculated using (2). The values of β_i were 0·0979, 0·0981 and 0·0983 for the three peaks at 31·6°, 34·35° and 36·2°, respectively. The corresponding values of β were 0·2331, 0·2069 and 0·2988, respectively. These values were converted to radians for particle size estimation. The values of particle size calculated using (1) comes out to be 37·74, 41·93 and 30·51 nm, respectively. The particle size was calculated taking $k = 0{\cdot}94$ (Choudhury and Sharma 1999; Gumus *et al* 2006) and $\lambda = 1{\cdot}5418$ Å, the wavelength of CuKα radiation. The average value of particle size taking instrumental broadening into account comes out to be 36·73 nm. The actual particle size will be a little higher than this since broadening due to strain was not taken into account while particle size was being calculated. Figure 3 shows TEM micrograph of ZnO powder scratched out from the film. Particle sizes ranging between 26 to 60 nm was observed in the TEM image with an average value of ~41 nm.

FWHM (β) values for Cd:ZnO films was found to increase with Cd incorporation. The average value of β in degrees for 5% Cd:ZnO and 10% Cd:ZnO are 0·2735 and 0·2899, respectively as opposed to 0·2427 for pure ZnO. The average particle sizes come out to be 32 nm and 29·9 nm, respectively for 5% and 10% Cd:ZnO, respectively using the corresponding values of β. Such broadening of X-ray diffraction peaks and decrease in grain size for Cd-doped films has been reported by Maiti *et al* (2007) and Vijayalakshmi *et al* (2008). These observations along with decrease in relative intensity of (002)

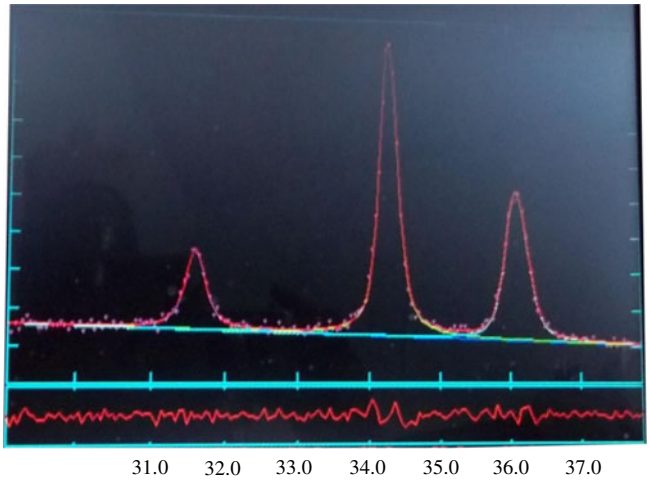

Figure 2. Observed (dotted) and simulated (continuous) X-ray diffraction patterns of ZnO.

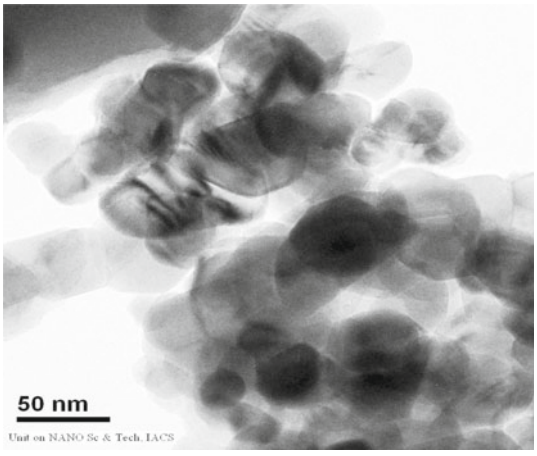

Figure 3. TEM image of ZnO.

peak confirms that Cd incorporation increases the degree of polycrystallinity of the films. The decrease in grain size with increasing Cd incorporation is possibly due to strain developed in the films due to Cd replacement (Maiti *et al* 2007). As explained in literature, such an increase of strain energy may lead to a loss of preferred orientation and enhancement of random orientation (Seel *et al* 1996; Lee *et al* 1998).

Figures 4(a)–(c) show SEM images of pure, 5% and 10% Cd:ZnO films, respectively. The images show a general view of the morphology of pure and Cd-doped ZnO films synthesized on glass substrate. The polycrystalline structure is revealed from the SEM micrographs. The films are porous as evident from absence of close packed morphology. The formation of sub-micrometer crystallites of varying sizes indicates agglomeration. Agglomeration of small crystallites in certain regions of the films is also evident from the figures. Such agglomeration makes it difficult to evaluate the grain size from SEM images. Some difference in surface morphology is observed for Cd:ZnO films [figures 4(b)–(c)] compared to pure ZnO [figure 4(a)]. It appears that the morphology gets less rougher for Cd:ZnO films.

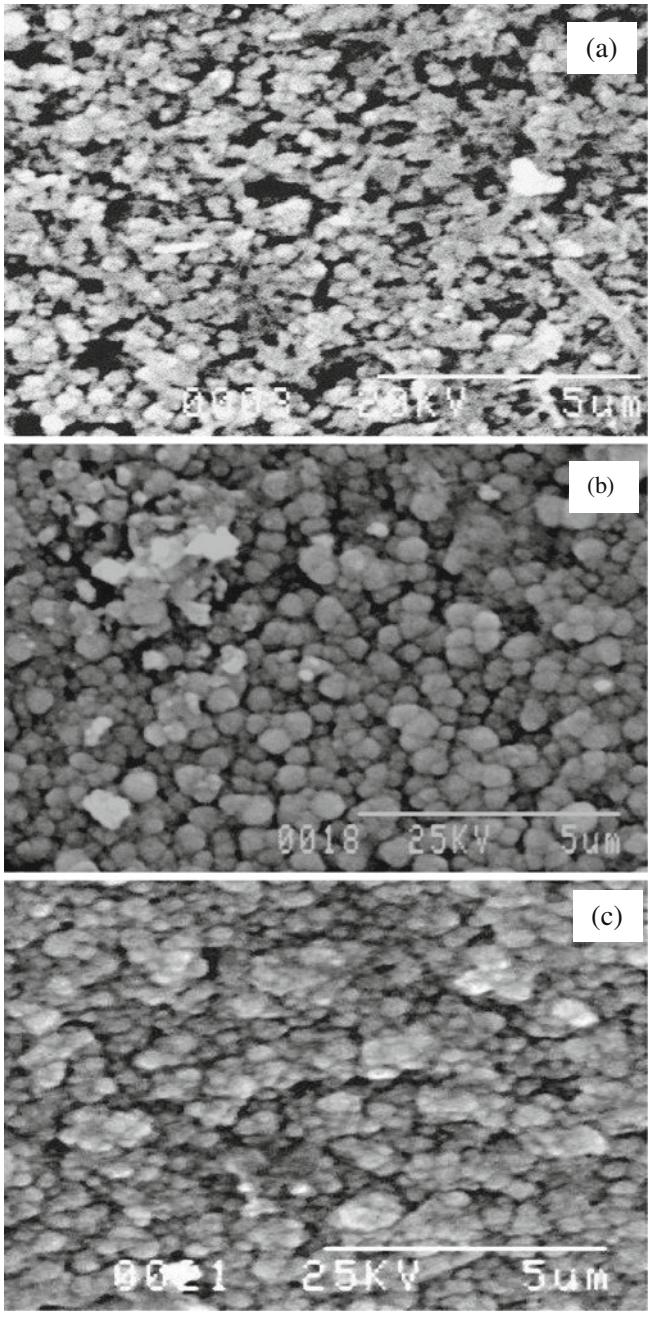

Figure 4. SEM images of (**a**) undoped ZnO, (**b**) 5% Cd:ZnO and (**c**) 10% Cd:ZnO.

The compositional analysis of Cd-doped ZnO film carried out by energy dispersive X-ray analysis is shown in figure 5. Figure 5(a) shows EDX spectrum of 5% Cd:ZnO and 5(b) shows the spectrum of 10% Cd:ZnO. EDX spectrum confirmed the presence of Zn, O and Cd elements in the deposited films. The silicon signal possibly appears from the substrate. Trace amount of carbon was also detected in the film. Dopant concentration in these two cases was 5% and 10% in the starting solution. Accordingly the expected Cd/Zn ratio was 0·05 and 0·1 in the films. We actually obtained the Cd/Zn ratio in the films as 0·0075 and 0·0185, respectively indicating that the amount of Cd incorporation in the film is much less than the amount of Cd in the starting solution. Details of EDX investigations on quartz substrate (to avoid silicon background signal) to evaluate the amount of Cd incorporation with varying Cd contents in the starting solution are underway. From the analysis of such a variation, it may be possible to impurify ZnO with any predetermined amount of Cd by this technique. The primary aim of the present investigation was to explore the possibility of doping ZnO with cadmium by SILAR. The present observation suggests that upon increasing the Cd concentration in the starting solution, the amount of Cd in the solid films increases. The low incorporation of Cd into the films (0·75% in the film against 5% in the starting solution for 5% Cd:ZnO film and 1·85% in the film against 10% in the starting solution for 10% Cd:ZnO film obtained from EDX measurements) may be due to mild working conditions of SILAR technique.

The optical absorption spectrum of the undoped ZnO and Cd-doped ZnO thin films was determined in a UV-VIS spectrophotometer (Shimadzu, Model UV-1800) spectrophotometer within the wavelength range of 200–500 nm. The spectra were measured by taking a similar glass as a reference on which film deposition was carried out and hence the spectra were from the films only. Both ZnO and CdO are considered as direct bandgap materials (Tabet-Derraz *et al* 2002). The energy gap (E_g) can thus be estimated by assuming direct transition between conduction band and valence bands. Theory of optical absorption gives the relationship between the absorption coefficient, α and the photon energy, $h\nu$ for direct allowed transition as

$$(\alpha h\nu)^2 = A\left(h\nu - E_g\right),$$

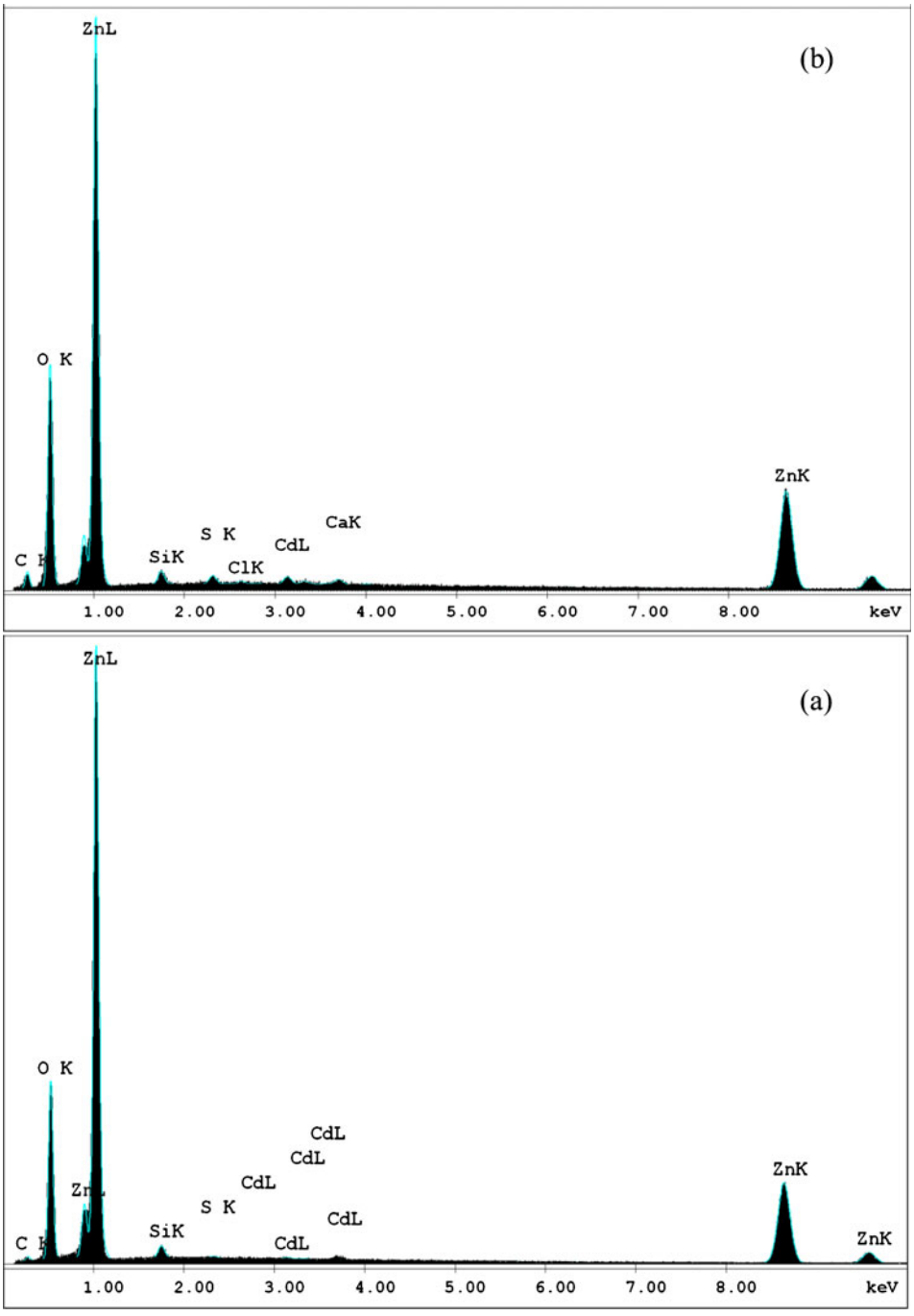

Figure 5. EDX pattern of (**a**) 5% Cd:ZnO and (**b**) 10% Cd:ZnO.

where A is a function of index of refraction and hole/electron effective masses (Pankove 1971). The direct bandgap is determined using this equation when straight portion of the $(\alpha h\nu)^2$ against $h\nu$ plot is extrapolated to intersect the energy axis at $\alpha = 0$. Plot of $(\alpha h\nu)^2$ against $h\nu$ for undoped and cadmium-doped ZnO films are shown in figure 6. Figure 6(a) shows the spectrum for pure ZnO while figures 6(b) and (c) show the spectrum for 5% Cd:ZnO and 10% Cd:ZnO, respectively.

It is seen that with the increase of cadmium-doping level, the fundamental absorption edge decreases. The value of E_g for undoped ZnO is 3·18 eV. It decreases to 3·14 eV for 5% Cd:ZnO and to 3·11 eV for 10% Cd:ZnO. This decrease can be accounted for by the large difference in E_g values of ZnO and CdO (Dong *et al* 1997; Cao *et al* 2000; Vigil *et al* 2000; Maiti *et al* 2007; Vijayalakshmi *et al* 2008). While Maiti *et al* (2007) reported a decrease in bandgap value from 3·29 eV for undoped ZnO to 3·15 eV for 6% Cd-doped ZnO,

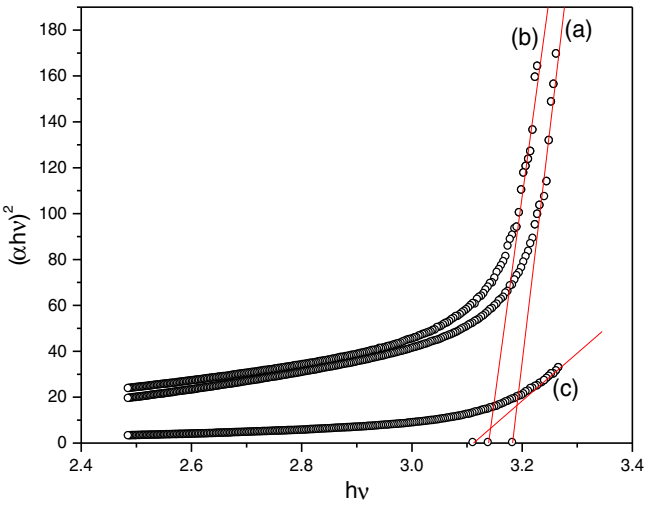

Figure 6. Photon energy (eV) dependence of (**a**) ZnO, (**b**) 5% Cd:ZnO and (**c**) 10% Cd:ZnO.

Vijayalakshmi *et al* (2008) reported a decrease from 3·12 eV for undoped to 2·96 eV for 25% Cd-doped ZnO.

4. Conclusions

Cadmium-doped ZnO films could be successfully synthesized through this simple chemical technique. The films had good adherence to the substrate. Apart from being an inexpensive and simple technique, the method uses milder reaction conditions than those employed by most chemical methods proposed in the literature. XRD spectra showed that the films are of hexagonal structure. Particle size evaluated using X-ray line broadening analysis shows a constantly decreasing trend with increasing cadmium incorporation. The average particle size of 36·73 nm evaluated by X-ray method neglecting line broadening matches well with TEM observation. The average particle size reduces to 32 nm for 5% Cd:ZnO and 29·9 nm for 10% Cd:ZnO. The films are polycrystalline and are of low density as evident from SEM micrographs. The polycrystallinity of the films increases with increasing Cd incorporation as evident from X-ray observations. These observations along with EDX observation confirm the replacement of zinc ion by cadmium ions in the ZnO lattice. Details of EDX investigation on quartz substrate with different Cd concentrations are underway to study the variation of amount of Cd incorporation in the films against the amount in the starting solution. With increase of Cd doping, the fundamental absorption edge changes. It decreases to 3·11 eV for 10% Cd:ZnO from 3·18 eV for pure ZnO. The materials are, therefore, useful for configurations that involved bandgap engineering. Cd-doped ZnO with polycrystalline and porous microstructures offers potential application as humidity sensors due to its large surface to volume ratio.

References

Aktaruzzaman A F, Sharma G L and Malhotra L K 1991 *Thin Solid Films* **198** 67

Al-zaidi Q G, Suhail A M and Al-azawi W R 2011 *Appl. Phys. Res.* **3** 89

Bedir M, Oztas M, Yazici A N and Kafadar E V 2006 *Chinese Phys. Lett.* **23** 939

Call R L, Jaber N K, Seshan K and Whyte J R 1980 *Solar Energy Mater.* **2** 373

Cao H, Xu J Y, Zhang D Z, Chang S H, Ho S T, Seeling E W, Liu X and Chang R P H 2000 *Phys. Rev. Lett.* **84** 558410

Chatterjee A P, Mitra P and Mukhopadhyay A K 1999 *J. Mater. Sci.* **34** 4225

Choi Y S, Lee C G and Cho S M 1996 *Thin Solid Films* **289** 153

Choudhury N and Sharma B K 1999 *Bull. Mater. Sci.* **32** 43

Dong L F, Cui Z and Zhang Z K 1997 *Nanostruct. Mater.* **8** 815

Ghosh S, Srivastava P, Pandey B, Saurav M, Bharadwaj P, Avasthi D K, Kabiraj D and Shivaprasad S M 2008 *Appl. Phys. A: Mater. Sci. Process.* **90** 765

Ghosh B, Dutta H and Pradhan S K 2009 *J. Alloys Compds* **479** 193

Gruber Th, Kirchner C, Kling R, Reuss F, Waag A, Bertram F, Forster D, Christen J and Schreck M 2003 *Appl. Phys. Lett.* **83** 3290

Gumus C, Ozkendir O M, Kavak H and Ufuktepe Y 2006 *J. Optoelectron. Adv. Mater.* **8** 299

Gupta M, Sharma V, Shrivastava J, Solanki A, Singh A P, Satsangi V R, Dass S and Shrivastav R 2009 *Bull. Mater. Sci.* **32** 23

Jumin X and Wang J 2001 *Mater. Lett.* **49** 318

Klug H P and Alexander L E 1974 *X-ray diffraction procedures for polycrystalline and amorphous materials* (New York: Wiley)

Kumar R, Singh A P, Thakur P, Chae K H, Choi W K, Angadi B, Kaushik S D and Patnaik S 2008 *J. Phys. D: Appl. Phys.* **41** 155002

Lee Y E, Kim Y J and Kim H J 1998 *J. Mater. Res.* **13** 1260

Maiti U N, Ghosh P K, Ahmed F, Mitra M K and Chattopadhyay K K 2007 *J. Sol–Gel Sci. Technol.* **41** 87

Makino T, Segawa Y, Kawasaki M, Ohtomo A, Shiroki R, Tamura K, Yasuda T and Koinuma H 2001 *Appl. Phys. Lett.* **78** 1237

Mandal S K and Nath T K 2006 *Thin Solid Films* **515** 2535

Mitra P and Khan J 2006 *Mater. Chem. Phys.* **98** 279

Mondal S, Kanta K P and Mitra P 2008 *J. Phys. Sci.* **12** 221

Nicolau Y F, Dupuy M and Brunel M 1990 *J. Electrochem. Soc.* **137** 2915

Pankove J I 1971 *Optical processes in semiconductors* (Englewood Cliffs, NJ: Prentice- Hall)

Patra S, Mitra P and Pradhan S K 2011 *Mater. Res.* **14** 17

Ristov M, Sinadinovski G J, Grozdanov I and Mitreski M 1987 *Thin Solid Films* **149** 65

Seel S C, Carel R and Thompson C V 1996 *Polycrystalline thin films: Structures, textures, properties and applications II* (Pittsburg, PA: Mater. Res. Symp. Proc.)

Suchea M, Christoulakis S, Katsarakis N, Kitsopoulos T and Kiriakidis G 2007 *Thin Solid Films* **515** 6562

Tabet-Derraz H, Benramdane N, Nacer D, Bouzidi A and Medles M 2002 *Sol. Energy Mater. Solar Cells* **73** 249

Vigil O, Vaillant L, Cruz F, Santana G, Morales-Acevedo A and Contreras-Puente G 2000 *Thin Solid Films* **361** 53

Vijayalakshmi S, Venkataraj S and Jayavel R 2008 *J. Phys. D: Appl. Phys.* **41** 245403

Wang F Z, Ye Z Z, Ma D W, Zhu L P, Zhuge F and He H P 2005 *Appl. Phys. Lett.* **87** 143101

Yakuphanoglu F, Ilican S, Caglar M and Caglar Y 2010 *Superlattice Microstruct.* **47** 732

Yogeeswaran G, Chenthamarakshan C R, Tacconi N R and Rajeshwar K 2006 *Mater. Res. Soc.* **21** 2334